



## Using a new phase-locked visual feedback protocol to affirm simpler models for alpha dynamics



Xingyi Jin <sup>a,b,1</sup>, Zhiguo Zhang <sup>a,b,c,d,1</sup>, Li Zhang <sup>a,b</sup>, Linling Li <sup>a,b</sup>, Gan Huang <sup>a,b,\*</sup>

<sup>a</sup> School of Biomedical Engineering, Health Science Center, Shenzhen University, Shenzhen, Guangdong 518060, China

<sup>b</sup> Guangdong Provincial Key Laboratory of Biomedical Measurements and Ultrasound Imaging, Shenzhen, Guangdong 518060, China

<sup>c</sup> Marshall Laboratory of Biomedical Engineering, Shenzhen University, Shenzhen 518060, China

<sup>d</sup> Peng Cheng Laboratory, Shenzhen, Guangdong 518055, China

### ARTICLE INFO

#### Keywords:

Endogenous alpha oscillations  
Exogenous visual stimulus  
Phase-locked visual feedback (PLVF)  
Neural modulation

### ABSTRACT

Alpha band oscillations are the most prominent rhythmic oscillations in EEG, which are related to various types of mental diseases, such as attention deficit hyperactivity disorder, anxiety, and depression. However, the dynamics of alpha oscillations, especially how the endogenous alpha oscillations be entrained by exogenous stimulus, are still unclear. Recently, a newly-developed phase-locked visual feedback (PLVF) protocol has shown effectiveness in modulating alpha rhythm, which provides empirical evidence for the further investigation of the neural mechanism of alpha dynamics. In this work, extensive numerical simulations based on four well-studied models were used to investigate the questions that (1) What kind of dynamic model exhibits a modulation phenomenon of PLVF? (2) What is the dynamic mechanism of PLVF for alpha modulation? (3) Which factors affect the modulation effects in PLVF? The result indicates that the dynamics of endogenous alpha oscillations are close to a simpler dynamic structure, like fixed-point attractor or limit-cycle attractor, which shows a global consistent dynamic behavior at different phases of the alpha oscillation. The further analysis explains the dynamic mechanism of PLVF for amplitude and frequency modulation of the alpha rhythm, as well as the influence of parameter settings in the modulation. All these findings provide a deeper understanding of the endogenous alpha oscillations entrained by exogenous phased locked visual stimulus and lead in turn to the refinement of a control strategy for alpha modulation, which could potentially be used in developing new neural modulation methods for cognitive enhancement and mental diseases treatment.

### 1. Introduction

Discovered by Hans Berger in 1924, alpha rhythm (8–12 Hz) is the earliest recorded human brain rhythm, which is the most prominent rhythmic oscillation in Electroencephalography (EEG) (Cohen, 2017; Ince et al., 2020). Many studies have shown that alpha rhythm is highly related to several types of cognitive functions (Debener et al., 2006; Hanslmayr et al., 2005), like memory (Hsueh, 2017; Maltseva and Masllobov, 1997) and attentional (Hanslmayr et al., 2011). Abnormal alpha rhythm is often related to various types of mental diseases, such as attention deficit hyperactivity disorder (Butnik, 2005; Fox et al., 2005), anxiety (Hammond, 2005), and depression (Choi et al., 2011). Hence, the modulation of alpha rhythm has raised the fascinating prospect of brain functions enhancement and mental disease treatment. Common

approaches of non-invasive neural modulation, like transcranial electrical or magnetic stimulation (TES or TMS), can directly modulate alpha rhythm by delivering external stimuli. However, the strong electromagnetic artifacts during the exogenous stimulation (Noury and Siegel, 2017; Noury et al., 2016) have made the investigation of the modulation mechanism and the inter-subject response variability difficult, and the large response variability has limited the use of these techniques.

In the previous work, Huang et al. (2019) has proposed phase-locked visual feedback (PLVF) protocol for robust artifact-free alpha rhythm modulation. Stimulated by visual flashing, instead of electrical or magnetic stimulation, no electromagnetic artifact would be induced, which makes it possible for online detecting the phase of alpha rhythm and delivering transient visual stimulation at a specific phase to make a closed-loop alpha rhythm modulation. In result, consistent periodic joint

\* Correspondence to: School of Biomedical Engineering, Health Science Center, Shenzhen University, Shenzhen 518060, China.

E-mail address: [huanggan1982@gmail.com](mailto:huanggan1982@gmail.com) (G. Huang).

<sup>1</sup> They contributed equally to this paper

amplitude-frequency modulation effects have been shown on all subjects in the resting state with eyes open. More detail about the schema of the PLVF system and modulation results of PLVF in real EEG data would be introduced in Section 2.2 and Fig. 1. However, the real dynamic of alpha oscillation is still somewhat a black box for researchers. The uncertainty of internal dynamic structure and parameters in the real EEG modulation hinders our further exploration of the dynamic mechanism for the alpha modulation. The questions mainly focus on the following three points. Below, the problems have been summarized in three aspects.

Firstly, what kind of dynamic model exhibits a modulation phenomenon of PLVF? Generated by thalamo-cortical interaction (Lopes da Silva et al., 1980; Vijayan and Kopell, 2012; Bollimunta et al., 2011; Schreckenberger et al., 2006), alpha rhythm in both visual and somatosensory cortex propagates from higher-order to lower-order areas (Halgren et al., 2019) and can be detected from the occipital lobe during the resting state and has an increased amplitude when the eyes are closed (Kirschfeld, 2005). Since the discovery of alpha rhythm, various mathematical models have been developed to simulate alpha rhythm. Among these models, Jansen's neural mass model (Jansen et al., 1993; Grimbart and Faugeras, 2006) is widely used for its simplicity in describing the alpha rhythm generation. As a macroscopic-level model for alpha dynamic analysis, the neural mass model exhibits multiple dynamic behaviors with different parameter settings, including fixed-point, limit-cycle, and chaotic strange attractors (Huang et al.,

2011). cccc is generated in neuronal networks as a form of filtered noise. Glass et al. (1993), Palus (1993) and Stam et al. (1999) found that alpha rhythm cannot be distinguished from filtered noise. Others believe alpha rhythm is the product of spontaneous oscillation of the brain network, and that its realization is dominated by regular oscillations accompanied by irregular oscillations (Lopes da Silva et al., 1997). In addition, some evidence showed that EEG signals exhibit chaotic behaviors (Pereira et al., 2005; Zhang, 2017). Hence, the modulation phenomenon of PLVF provides us a probe to investigate the dynamics structs of alpha oscillation.

Secondly, What is the dynamic mechanism of PLVF for alpha modulation? Entrainment of the brain oscillations is commonly used to explain the modulation mechanism of repeated brain stimulation techniques, like rTMS and tACS (Schwab et al., 2006). But the strong electromagnetic artifacts make the investigation difficult. For the proposing of PLVF, the authors assumed the alpha oscillation as a simple pendulum model. In result, the modulation effect on the amplitude of alpha rhythm was the same as expected, but the joint amplitude-frequency modulation was not expected. Furthermore, the undamped simple pendulum model is not stable, and it cannot achieve a stable modulation effect with the PLVF protocol. With the understanding about the dynamics structs of alpha rhythm in the first question, how about the dynamic mechanism to produce the joint amplitude-frequency modulation result, especially how the endogenous alpha oscillations be entrained by exogenous

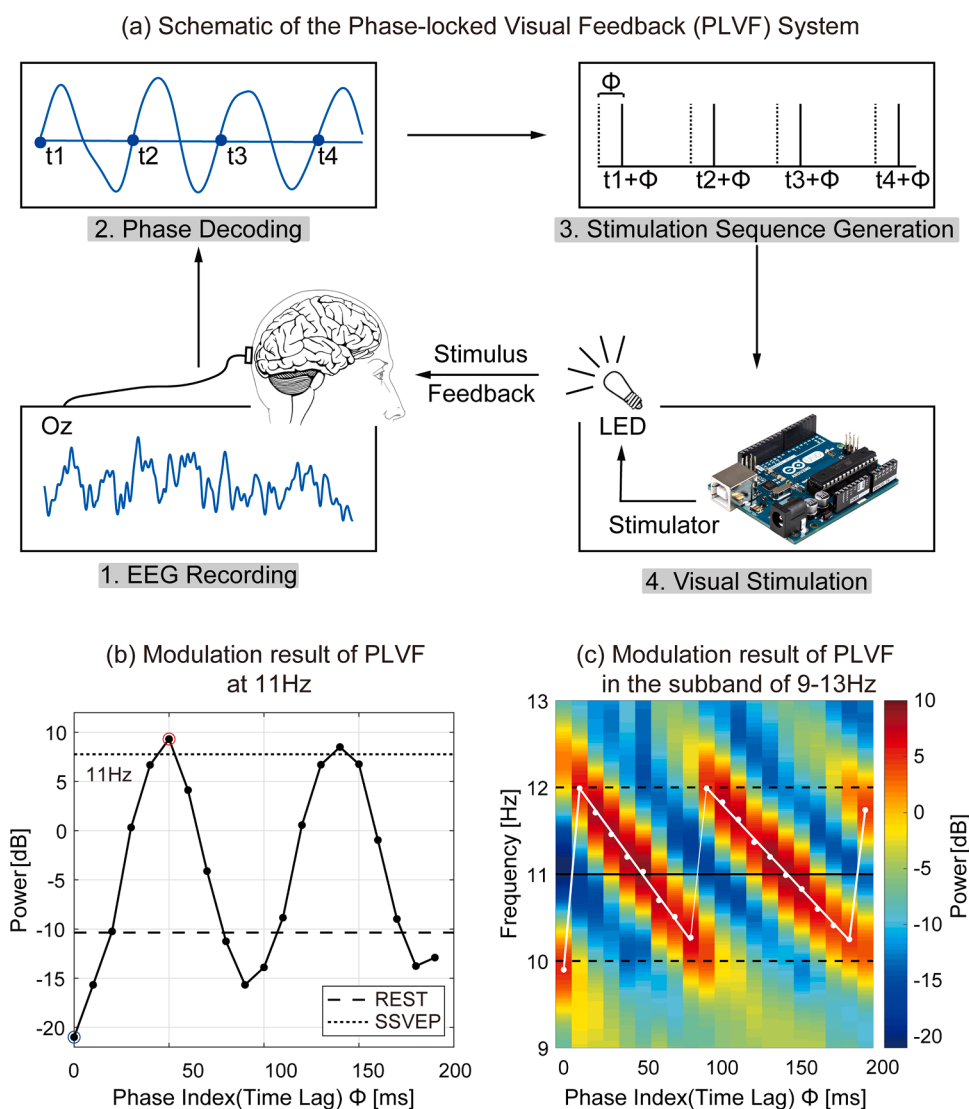


**Fig. 1.** Schema of PLVF system and modulation results of PLVF in real EEG data: (a) Schema of PLVF system; Raw EEG signals are firstly recorded and filtered, and then the phase of the alpha wave is detected which is used for the generation of visual stimulation sequence (i.e., the exact time to deliver visual stimuli). Finally, visual stimuli were delivered by LED to provide feedback to users. (b) The modulation effect of power shows a sinusoidal-like shape at 11 Hz of the real EEG data, in which the dash line indicates the power of alpha rhythm in resting state with eyes open without modulation, the dots line indicates the power of the SSVEP at 10 Hz. The valley and peak of the modulation function are marked by blue and red circles. (c) Joint amplitude-frequency modulation effect of PLVF in real EEG data (online EEG modulation). As the phase index  $\phi$  varies, the modulation effect at the peak frequency has clear periodicity, in which the peak frequency indicates the frequency with the biggest power in the alpha band. (For interpretation of the references to colour in this figure, the reader is referred to the web version of this article.)

(Reprinted from Huang et al. (2019), Copyright (2019), with permission from Elsevier).

stimulus, is one of the main concerns to investigate the alpha dynamics.

Thirdly, which factors affect the modulation effects in PLVF? Due to the uncertainty of internal dynamic structure and parameters, it is not easy to find the factors which potentially affect the modulation effects. To test the modulation result with different parameters is achievable in the numerical simulation but would be time-consuming in a real EEG experiment. Furthermore, the intra-subject variability caused by the nonstationary internal parameters would make the modulation result noisy. Based on the understanding of the dynamic structure and the modulation mechanism, we can further explore the factors affecting the modulation effect by numerical simulation. The results would in turn lead us to refine the control strategy for alpha modulation.

In this work, focusing on the questions of (1) What kind of dynamic model exhibits a modulation phenomenon of PLVF? (2) What is the dynamic mechanism of PLVF for alpha modulation? (3) Which factors affect the modulation effects in PLVF? Numerical simulations were applied on the neural mass model and three types of typical dynamic attractors including fixed-point, limit-cycle, and chaotic strange attractors to investigate the dynamics mechanism of alpha rhythm modulation by PLVF. The remainder of this paper is structured as follows. Section 2 introduces the PLVF system and the four dynamic models for the simulation of alpha rhythm modulation. Methods to investigate the dynamic mechanism of alpha modulation are described in Section 3. Simulation results are given in Section 4, while discussion and conclusions are provided in Section 5.

## 2. PLVF system and simulation models

### 2.1. Closed-loop neural modulation

Common approaches of non-invasive neural modulation, like transcranial electrical or magnetic stimulation (tES or TMS), can directly modulate alpha rhythm by delivering external stimuli. However, strong electromagnetic artifacts during the exogenous stimulation process (Noury and Siegel, 2017; Noury et al., 2016) make real-time monitoring of alpha rhythm difficult, which makes closed-loop modulation difficult. Although many methods were proposed to remove the artifacts online or offline, few of them have been widely accepted (Kasten and Herrmann, 2019). To address this issue, one approach was often adopted that the intermittent stimulation was immediately exerted when intermittent EEG recordings were paused and immediately analyzed (Beliaeva et al., 2021). Take transcranial alternating current stimulation (tACS), several such studies were published. Mansouri et al. (2018) used different phases of pulsed transcranial current to modulate theta and alpha oscillations according to the previous short-time oscillation phase. Zarubin et al. (2020) utilized 1 s tACS after analyzing previous 1 s oscillations to modulate alpha oscillations. Unfortunately, the modulation effects were often hard to interpret, which may be due to many factors such as the inherent delay of the system or the task design. Hence, it is quite hard now for tES or TMS for a real-time stimulation parameters adjustment to modulate the frequency or the phase of the individual neural oscillations to develop a closed-loop system (Frohlich and Townsend, 2021).

### 2.2. PLVF system

Compared with tES / TMS technique, visual stimuli can modulate the brain rhythm without any electromagnetic artifacts. To achieve closed-loop alpha modulation and realize more precise alpha modulation, Huang et al. (2019) propose a PLVF protocol for alpha rhythm modulation based on a simple pendulum assumption in the previous work. By delivering visual stimuli at different phases, PLVF modulation can induce different amplitude and frequency responses of the alpha rhythm. As shown in Fig. 1a, the schema of the proposed PLVF modulation includes four modules, which are EEG recording, phase decoding, stimulation sequence generation, and visual stimulation. Because the sequence of visual stimuli was generated based on the alpha phase and

then, in turn, modulated the alpha wave, closed-loop control of the alpha wave was formed.

- **Module 1 EEG recording.** The raw EEG signal is online recorded by Self developed C++ programmed from channel Oz with the sampling rate of 5000 Hz and referenced to FCz.
- **Module 2 Phase decoding.** To achieve real-time phase detection, the real-time EEG signal is firstly online filtered by a 2-order alpha-band (8–12 Hz) Butterworth bandpass filter. And then a zero-crossing point detection method is used on the filtered alpha rhythm to identify the positive zero-crossing points with phase  $3\pi/2$ .
- **Module 3 Stimulation sequence generation.** A certain time lag  $\phi$  (phase index) is introduced to estimate the time point of the alpha rhythm at other phases. Since the alpha rhythm has a period of around 100 ms, it is expected that the modulation effect on the alpha power with a different phase index  $\phi$  also varies in a period of around 100 ms.
- **Module 4. Visual stimulation.** A visual stimulation sequence is generated to be delivered at one fixed phase for each period of the alpha rhythm, which leads to closed-loop alpha rhythm modulation.

In the result shown in Fig. 1b and c, the amplitude of alpha rhythm shows a periodic change with the stimulation phase index  $\phi$ . As phase index  $\phi$  increases, the peak frequency of the modulated alpha rhythm periodically moves toward the lower-frequency bands. A more complete description of the PLVF system and modulation results can be found in Huang et al. (2019).

### 2.3. Dynamic model of PLVF

The dynamic model of the PLVF system can be described by a differential equation,

$$X' = F(X) + Ku(\tilde{y}, \phi), \quad (1)$$

where  $X$  is the state variable as a function of time  $t$ ,  $y$  is the observation representing the recorded EEG signal in the PLVF system,  $\tilde{y}$  is the online filtered signal of  $y$ ,  $\phi$  is the time lag, and  $K$  is a vector containing the stimulus direction and intensity.  $F(X)$  represents the endogenous evolution of the alpha rhythm, which can be described by different models for simulation.  $u(\tilde{y}, \phi)$  is the exogenous stimulus in the PLVF system. As a sum of impulse functions,  $u(\tilde{y}, \phi)$  depends on the filtered EEG signal  $\tilde{y}$  and the introduced time lag  $\phi$ . The  $m^{\text{th}}$  positive zero-crossing time point of the filtered signal  $\tilde{y}$  is detected as  $t_m$ , with  $\tilde{y} = 0$  and  $\tilde{y}' > 0$ . A time lag  $\phi$  is added to  $t_m$  to produce the phase at which the stimuli are delivered. Hence  $u(\tilde{y}, \phi)$  can be written as

$$u(\tilde{y}, \phi) = \sum_m \delta(t - (t_m + \phi)), \quad (2)$$

where  $\delta(t)$  is the unit impulse function with

$$\int_i^j \delta(t) dt = \begin{cases} 1, & i < 0 < j, \\ 0, & \text{otherwise.} \end{cases} \quad (3)$$

### 2.4. Dynamic models of the alpha rhythm

To further understand the dynamic of the alpha rhythm and the modulation mechanism of the PLVF system, different neural dynamic models are applied in this study. Previous work modeled the alpha rhythm as the motion trajectory of a simple pendulum without damping (Huang et al., 2019). But this is too simple to precisely describe the alpha rhythm, which is unstable with continuously delivered phase-locked stimuli in the PLVF system. To investigate the dynamic structures of alpha rhythm with joint amplitude-frequency modulation (Fig. 1b) in the PLVF system, four types of dynamical models are applied. The first

one is the neural mass model, which has been well studied for the generation of alpha oscillation (Huang et al., 2011). Since oscillation is the basic characteristic of the alpha rhythm, three typical types of oscillatory attractors are also used to simulate the alpha rhythm, which are the linear fixed-point attractor, nonlinear limit-cycle attractor, and chaotic strange attractor.

- Model 1: Neural mass model

At the cellular level, it is well known that the generation of EEG relies on the interactions within or between neurons in the excitatory and inhibitory populations. Jansen's neural mass model (Huang et al., 2011; Jansen and Rit, 1995) can simulate the interaction of excitatory and inhibitory populations. In this model, the neural population is simulated by a population of pyramidal cells, and the output is subject to excitatory and inhibitory synaptic control. The state variable  $X$  is a six-dimensional vector,  $X = [x_1, x_2, x_3, x_4, x_5, x_6]^T$ , with the initial value randomly selected from the interval  $x_1 \in [0.1, 0.13]$ ,  $x_2 \in [23.6, 24]$ ,  $x_3 \in [14.5, 18]$ ,  $x_4 \in [-1.4, 1.3]$ ,  $x_5 \in [-14, 10.5]$ ,  $x_6 \in [-108, 110]$ , since the attractor located in the region. The output  $y = x_2(t) - x_3(t)$ , the stimuli intensity  $K = [0, 0, 0, 0, 3000, 0]^T$ , and

$$F_1(X) = \begin{bmatrix} x_4 \\ x_5 \\ x_6 \\ \text{Sigm}(x_2 - x_3) - 2ax_4 - a^2 x_1 \\ AaC_2 \text{Sigm}(C_1 x_1) - 2ax_5 - a^2 x_2 + Aap \\ BbC_4 \text{Sigm}(C_3 x_1) - 2bx_6 - b^2 x_3 \end{bmatrix}, \quad (4)$$

where  $\text{Sigm}(v)$  is the nonlinear sigmoid function,

$$\text{Sigm}(v) = \frac{2e_0}{1 + e^{s(v_0-v)}}, \quad (5)$$

and the parameter settings are

$$\begin{aligned} A &= 3.25mV, \quad a = 100s^{-1} \\ B &= 22mV, \quad b = 50s^{-1} \\ e_0 &= 2.5s^{-1}, s = 0.56mV^{-1}, v_0 = 6mV \\ C_1 &= 1.25C_2 = 4C_3 = 4C_4 = C. \end{aligned}$$

With  $p = 200$  and  $C = 135$ , the output of neural mass model  $y = x_2 - x_3$  shows typical alpha-like activity.

- Model 2: Fixed-point attractor

According to the theory that alpha rhythm is generated by the filtering of brain noise, a noise-driven linear point attractor is established. The state variable for this model is a two-dimensional vector,  $X = [x_1, x_2]^T$ , with the initial value randomly selected from the interval  $x_1 \in [-2, 2], x_2 \in [-2, 2]$ , since the attractor is located in the region. The output  $y = x_1$ , the stimulus intensity  $K = [3000, 0]^T$ , and

$$F_2(X) = \begin{bmatrix} m & n \\ -n & m \end{bmatrix} X + \epsilon, \quad (6)$$

where  $\epsilon$  is Gaussian white noise with mean 0 and variance 100. The value of  $m$  indicates the rate of convergence of the system, and  $n$  indicates the rhythm of the oscillation. With  $m = -10$  and  $n = 70$ , the output of the point attractor model  $y = x_1$  shows an alpha-like activity with a peak frequency around 11 Hz.

- Model 3: Limit-cycle attractor

According to the theory that alpha rhythm is generated by the spontaneous oscillation of the brain's neural network, a nonlinear limit-cycle attractor with constant angular velocity is established. It

is a simple close orbit with periodic oscillation. The state variable is a two-dimensional vector,  $X = [x_1, x_2]^T$ , with the initial value randomly selected from the interval  $x_1 \in [-1.5, 1.5], x_2 \in [-1.5, 1.5]$ , since the attractor is located in the region. The output  $y = x_1$ , the stimulus intensity  $K = [3000, 0]^T$ , and

$$F_3(X) = \begin{bmatrix} \frac{kx_1}{r} - kx_1 - cx_2 \\ \frac{kx_2}{r} - kx_2 + cx_1 \end{bmatrix}, \quad (7)$$

where the limit cycle trajectory is a circle with radius  $r = \sqrt{x_1^2 + x_2^2}$ . The value of  $k$  determines the rate of system convergence, and  $c$  determines the angular velocity, which is constant. With parameters  $k = 10, c = 60$ , the output of the limit-cycle attractor  $y = x_1$  shows an alpha-like activity.

- Model 4: Chaotic strange attractor

According to the theory that the irregularity of alpha rhythm may be related to the chaotic processes of the brain, the Lorenz attractor is established. This nonlinear chaotic attractor was obtained by meteorologist Edward Lorenz when he studied atmospheric convection in weather forecasting. It is a complex fractal orbit characterized by unstable, driving orbits. The state variable is a three-dimensional vector,  $X = [x_1, x_2, x_3]^T$ , with the initial value randomly selected from the interval  $x_1 \in [-130, 134], x_2 \in [-169, 176], x_3 \in [30, 300]$ , since the attractor is located in the region. The output  $y = x_3$ , the stimulus intensity  $K = [0, 0, 100000]^T$ , and

$$F_4(X) = \begin{bmatrix} -\sigma x_1 + \sigma x_2 \\ \gamma x_1 - x_2 - x_1 x_3 \\ x_1 x_2 - d x_3 \end{bmatrix}, \quad (8)$$

where  $\sigma = 80$  is the Prandtl number,  $\gamma = 180$  is the Rayleigh number, and  $d = 25$  is a velocity damping constant.

### 3. Methods

Aiming to understand the alpha dynamics behind the joint amplitude-frequency alpha modulation in the PLVF system, four dynamic models are used for a simulation study. Compared to the chaotic strange attractor and the neural mass model, which dynamic are complex, and the noise-driven fixed-point attractor, which contains noise and makes the explanation of the dynamic difficult, the limit-cycle attractor has a simpler dynamic structure. Hence, it is then used to investigate the underlying dynamic mechanism of PLVF modulation. Finally, we analyze parameters in the model to find out key factors that may affect the results.

#### 3.1. The method of numerical simulation

The Runge-Kutta method is applied in the simulation to solve Eq. (1). The simulation time is 200 s, the sampling rate is 1000 Hz, and the iteration step is 0.001 s. Parameter settings of the four models are shown in Section 2.3. In the first 40 s, there is no stimulation, so that the model can enter a stable state. External stimuli are applied from the 40th second to realize phase-locked modulation. The output signal of the model (simulated EEG signal) is recorded for power spectrum analysis, which is performed within 100–200 s of the output signal using Welch's method, with a window width of 5000, overlapping of 50%, and frequency ranging from 6 Hz to 15 Hz in steps of 0.01 Hz. All simulation and analyses are carried out using MATLAB R2020a software on a Hewlett-Packard ProDesk computer with an Intel i7-6700 CPU at 3.4 GHz. Considering the different initial values, all in the simulation have been repeated 10 times. For each model, the modulation results of each time in two specific phases are shown to illustrate the influence of the set of the initial values (Neural mass model:  $\phi = 50, 120$  ms; Fixed-

point attractor:  $\phi = 55, 100$  ms; Limit cycle attractor:  $\phi = 80, 100$  ms; Lorenz attractor:  $\phi = 70, 100$  ms). Meanwhile, the representative phases for each model are chosen, which corresponds to the inhibition and enhancement modulation effects.

### 3.2. The analysis of alpha modulation effects

For simplicity of analysis, the limit-cycle attractor is used to investigate the underlying neurodynamic mechanism of the PLVF system. The phase portraits of PLVF modulation at time lag  $\phi = 10$  ms and  $\phi = 80$  ms are illustrated to explain the dynamic mechanism of amplitude and frequency modulation. The PLVF modulation result is described with the increase of phase index  $\phi$  from 0 to 200 ms. The phase portraits with phase index  $\phi = 10, 45, 80, 115, 150$ , and 185 ms are used to describe the dynamics of neural modulation with the increase of phase index. The power and frequency modulation with the increase of phase index are explained to summarize the dynamic mechanism of PLVF.

### 3.3. The influence of parameters setting

A signal simulated by a neural mass model, or a limit-cycle attractor cannot precisely simulate real alpha rhythm due to purity. Considering the complex dynamics of the neural mass model and strange attractor, the dynamics of a noise-driven fixed-point attractor are relatively simple. Therefore, the fixed-point attractor is chosen to investigate the factors affecting the modulation results. Four factors are under investigation, and they are stimulus intensity, the bandwidth of the bandpass filter, the center frequency of the bandpass filter, and the accuracy of phase estimation.

In online EEG modulation, the stimulation intensity is an important parameter, which should be large enough to produce an evident modulation effect, but may make participants feel uncomfortable when it is too large. Hence, we consider stimulation intensity as an important factor to investigate the effects of modulation results. Furthermore, because the peak frequency of alpha rhythms differs between individuals (Grandy et al., 2013), the setting of the bandpass filter (center frequency and filter bandwidth) may have a great influence on the modulation results. Therefore, we examine the influence of a bandpass filter with: (1) fixed center frequency and variable filter bandwidth; and (2) fixed filter bandwidth and variable center frequency. In addition, the accuracy of phase estimation is important to PLVF modulation to ensure the modulation effect because, when stimulated at different phases, alpha rhythms have different dynamic responses and modulation effects (Brandt, 1997). Therefore, the accuracy of phase estimation is another important factor to explore. The initial value is randomly selected from the interval  $x_1 \in [-2, 2]$ ,  $x_2 \in [-2, 2]$ . The parameter settings are as follows.

#### (1) Stimulation intensity

In the simulation, the stimulation intensity increases from 0 to 5000 with a step of 1000. The amplitude modulation range is estimated to show the modulation effect of stimulation intensity, which is calculated based on the minimum and maximum amplitude of the alpha rhythm during modulation.

#### (2) Bandwidth of bandpass filter

In the simulation, the bandwidth of the bandpass filter is set to 6–16 Hz, 7–15 Hz, 8–14 Hz, 9–13 Hz, and 10–12 Hz, with the center frequency fixed at 11 Hz. The frequency modulation range is estimated to show the modulation effect of filter bandwidth, which is calculated based on the minimum and maximum peak frequency during modulation.

#### (3) Center frequency of bandpass filter

In the simulation, the center frequency increases from 8 Hz to 12 Hz, with an interval of 1 Hz. The filter bandwidth is fixed at 2 Hz. The frequency modulation range is estimated to show the modulation effect of the center frequency, which is also

calculated based on the minimum and maximum peak frequency during modulation.

#### (4) Accuracy of phase estimate

Since the error in phase estimation is inevitable in real EEG modulation by PLVF, which will increase with the phase index, the phase estimate accuracy is considered in this simulation, with the form

$$\tilde{\Phi} = \Phi(1 + e_i R_d), \quad (9)$$

where  $\Phi$  is the real phase index,  $R_d$  is a random number from a zero-mean normal distribution, and  $e_i$  is the error index, which increases from 0 to 1, with a step of 0.01. Here, we use  $\tilde{\Phi}$  with the error in the phase estimation instead of  $\Phi$  in Eq. (1). We set the parameter of the error index from 0 to 1, with an interval of 0.01. Due to the error of the phase estimation, the modulation effect of alpha power is attenuated with the phase index varies. Therefore, we use exponential fitting to fit the power modulation effect, and the fitting attenuation coefficient  $\mu$  is used to describe the attenuation of power as the phase index increases, which is used to assess the modulation effect of phase estimation accuracy. The fitting formula of the attenuation coefficient is

$$y = \xi e^{\mu x}, \quad (10)$$

where  $\mu$  is the fitted attenuation coefficient,  $\xi$  is a positive real number not equal to 1, the argument  $x$  is the phase index, and  $y$  is the fitted result.

## 4. Results

### 4.1. Simulation results in different models

The modulation effects on the amplitude and frequency of the alpha rhythm are shown in Figs. 2 and 3 for the four types of models.

The modulation result for the neural mass model is illustrated in Fig. 2a, which shows similar joint amplitude-frequency alpha rhythm modulation with the change of the stimulation phase. But this still differs from real EEG modulation. First, the peak frequency of the modulated alpha rhythm does not increase linearly with the increase of the phase index  $\phi$ . Furthermore, the peak of the power modulation effect (black dots in Fig. 2a) is at the lower frequency of the frequency modulation range, while it is in the middle frequency of the online EEG frequency modulation range (Fig. 1b). The nonlinearity of the neural mass model causes globally inconsistent dynamic characteristics, so the same force at different positions in the phase space leads to different effects on the system. The modulation results at different phase indexes ( $\phi = 50, 120$ ) have largely different shapes, as illustrated in the middle of Fig. 2a.

Compared to the neural mass model, the dynamic structures of the fixed-point and limit-cycle attractors are much simpler. The fixed-point attractor mode is a linear model with noise, in which all positions share the same dynamic characteristics. The negative real part of the eigenvalues of the matrix  $\begin{bmatrix} m & n \\ -n & m \end{bmatrix}$  shows the system would eventually reach the fixed point. However, the existence of noise prevents the convergence of the solution to the fixed points. The periodic oscillation with alpha rhythm is caused by the imaginary part of the eigenvalues in the simulation model. As illustrated in the middle of Fig. 2b, the modulation results of the fixed-point attractor are closer to the real online EEG modulation result in Fig. 1b. With phase-locked stimuli at different phases, the alpha rhythm induces different modulation results, while the phase portraits of modulation results at phase indexes  $\phi = 55, 100$  are too noisy to observe the modulation mechanism.

Without the influence of noise, the modulation result from the limit-cycle attractor is clearer and more regular in Fig. 2c. In the proposed limit-cycle attractor, the noise in the fixed-point model is replaced by a constant outward force, which makes the model nonlinear and more

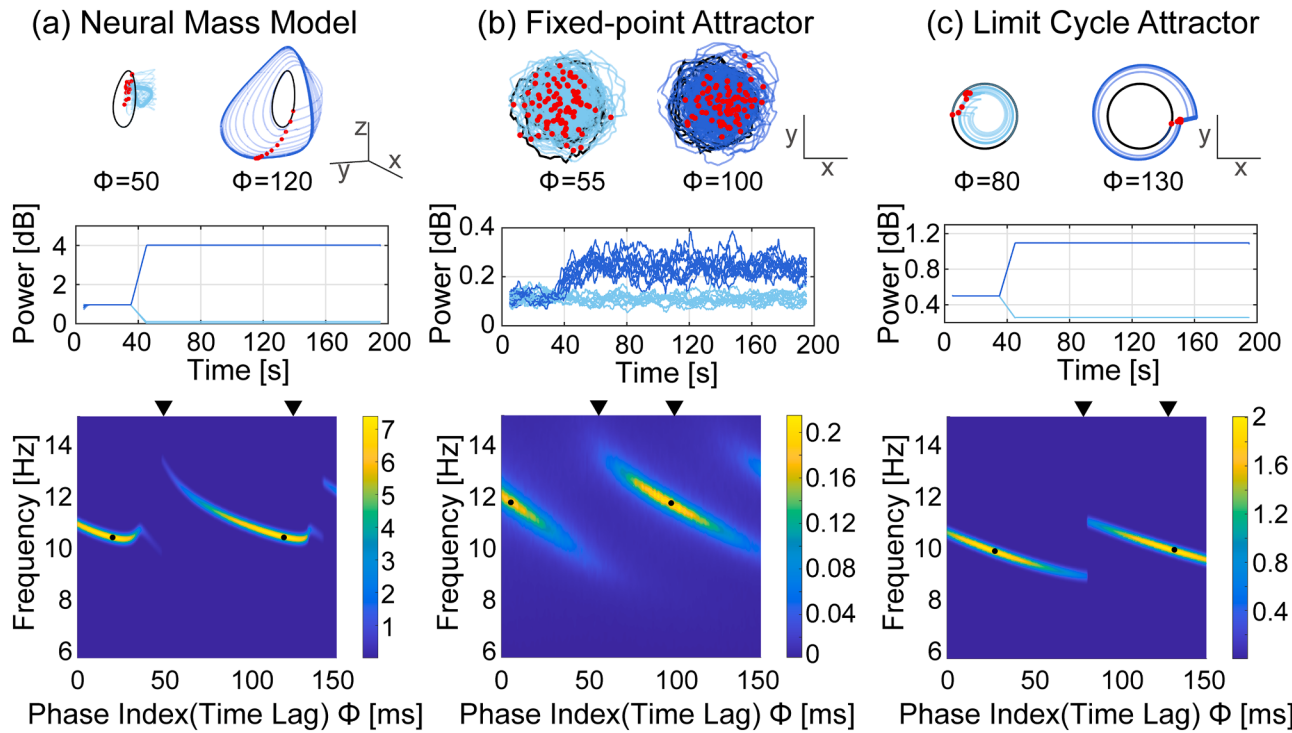


**Fig. 2.** Modulation results (amplitude and frequency modulation functions against phase index/time lag  $\phi = 0 - 150$  ms) of (a) the neural mass model, (b) the fixed-point attractor, and (c) the limit-cycle attractor. Phase portraits at the top raw are modulation trajectories with stimuli at the two different phase indexes (indicated by black triangles at x-coordinates of lower plots). The black curve indicates the resting state of the system from 38 to 40 s before the stimulus. And the blue curve indicates the modulated state of the system from 40 to 48 s after the stimulus. The results in the middle raw show the power changed with time with 10 different initial values and stimuli at the two different phase indexes. Considering a 10 s window is used for smoothing, all the results are shown from 5 to 195 s. Modulation results at the bottom show the joint amplitude and frequency modulation effect and are the average of the results of 10 different initial values. The black dots indicate the peak of the power modulation effect.(For interpretation of the references to colour in this figure, the reader is referred to the web version of this article.)

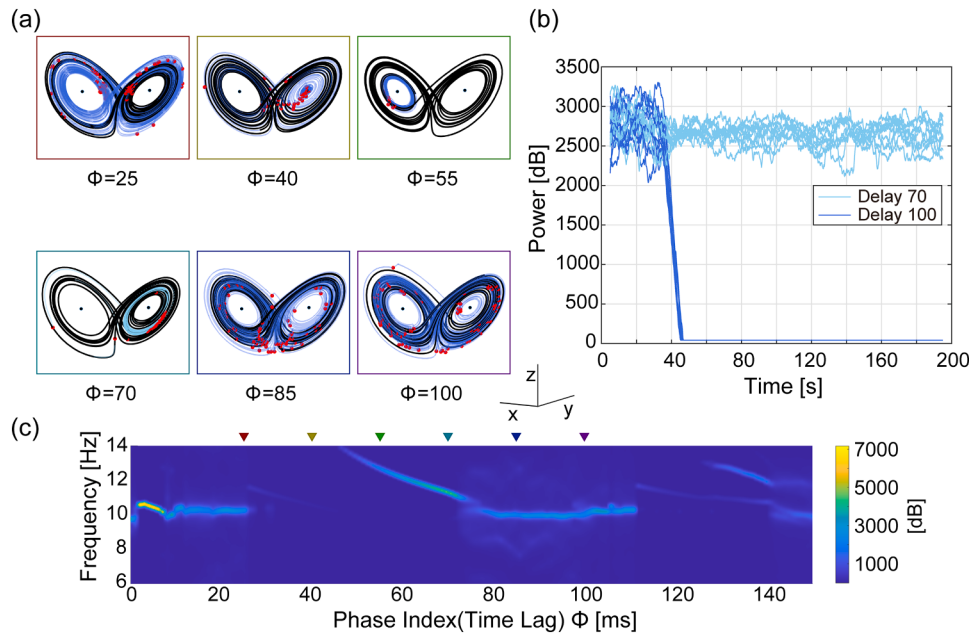


**Fig. 3.** Modulation results of Lorenz attractor: (a) Phase portrait of Lorenz attractor with phase index  $\phi = 25, 40, 55, 70, 85, 100$  ms. Black curves in phase portraits indicate trajectories without stimulation from 38 to 40 s before the stimulus. And blue curves indicate modulated trajectories from 40 to 48 s after the stimulus. Meanwhile, the black dots indicate two equilibrium points and the red circles indicate stimulation points; (b) The power response changes over time with 10 different initial values and stimuli at the phase index  $\phi = 70, 100$  ms; (c) The joint amplitude and frequency modulation effect against phase index (time lag)  $\phi = 0 - 150$  ms.(For interpretation of the references to colour in this figure, the reader is referred to the web version of this article.)

complex than the fixed-point attractor. But the dynamic characteristics of each point with the same radius are still very consistent. The phase portraits of the modulation result at phase indexes  $\phi = 80, 130$  are clearer, which is further investigated below in Section 4.2.

For the chaotic Lorenz attractor, the simulation shows a more complex modulation result in Fig. 3. It is interesting to find that it only has a

modulation effect like the online EEG modulation result under half-cycle phase index stimulation. With  $\phi = 40$ , the modulation effect is significant, and the oscillation behavior is greatly suppressed. With the increase of the phase index ( $\phi = 55, 70$ ), the radius of the modulation trajectory increases as the oscillation frequency decreases. At another half-period of the phase index ( $\phi = 25, 85, 100$ ), the modulation by PLVF

would no longer be effective.

For all four dynamic models, the difference of initial values does not influence the modulation results. To understand the modulation result of the chaotic Lorenz attractor, we analyze the dynamic characteristics near the fixed points. By setting  $F_4(X) = 0$  in Eq. (8), it is found that there is only one equilibrium point with  $r \leq 1$ , which is at the origin  $(0, 0, 0)$ . With  $r > 1$ , two additional equilibrium points appear, which are  $(\sqrt{b(r-1)}, \sqrt{b(r-1)}, r-1)$  and  $(-\sqrt{b(r-1)}, -\sqrt{b(r-1)}, r-1)$ . These two points are located in the center of the two wings of the butterfly trajectory. Bringing  $\sigma = 80$ ,  $\gamma = 180$ ,  $b = 25$  into the system, we find that the eigenvalues of the local linearization matrix

$$F'_4(X) = \begin{bmatrix} -\sigma & \sigma & 0 \\ r - x_3 & -1 & -x_1 \\ x_2 & x_1 & -b \end{bmatrix} \quad (11)$$

at the two nontrivial equilibrium points are  $\lambda_1 = -107.50$ ,  $\lambda_{2,3} = 0.75 \pm 81.61i$ . Hence the two nontrivial equilibrium points are unstable saddle points, but they have the same dynamic properties. Therefore, the trajectory in the system with phase index  $\phi = 40, 55, 70$  for PLVF modulation may be restricted in any one wing of the butterfly. As shown in Fig. 4 with  $\phi = 70$ , the modulation curve converges to the left-wing, or the right-wing, which depends on the initial value. But whatever in which wing the trajectory has the same amplitude and frequency response for a given phase index.

#### 4.2. Dynamic mechanism of PLVF modulation

To understand the joint amplitude-frequency modulation of PLVF in real EEG data, we first analyze the limit cycle model with the phase-locked stimulation at two phase indexes,  $\phi = 10ms$ , and  $\phi = 80ms$ , in Fig. 5. The simulation results of the PLVF system are shown in Fig. 6, as the phase index (time lag)  $\phi$  increases from 0 to 200 ms.

Fig. 5a shows the dynamics of the simulated EEG rhythm modulated by an external stimulus with phase index  $\phi = 10ms$ . The simulated raw EEG signal is first filtered by a second-order Butterworth filter with bandwidth 8–12 Hz. Zero-crossing detection is used to recognize the phase of  $3\pi/2$ , and a certain time lag  $\phi = 10ms$  is added to the zero-cross point to approximate the phase to be locked (upper left). The modulated EEG signal is illustrated in blue curves. Without the external stimulus, the system runs.

in a fixed orbit (black cycle at upper-right). With the external stimulus, the system reaches a stable state in less than one second, and both the power and frequency of the oscillation increase (Fig. 6b and c). As illustrated in the phase portrait (upper-right) of Fig. 5a, it is found that the external stimulus causes the radius of the trajectory to increase ( $\Delta r > 0$ ), and the power of the oscillation correspondingly increases

( $P \uparrow$ ). The instantaneous phase angle also increases ( $\Delta\theta > 0$ ), as does the frequency of the oscillation ( $F \uparrow$ ).

Fig. 5b shows the dynamics of the simulated system modulated by an external stimulus with phase index  $\phi = 80ms$ . The whole process of modulation is similar to that of Fig. 5a (upper-left). But the phase index  $\phi$  increases from 10ms to 80ms. In the results, both the power and frequency of the oscillation decrease with external stimulation (Fig. 6b and c). Because the stimuli are delivered at different phases, it is found that the external stimuli decrease the trajectory radius ( $\Delta r < 0$ ), and the power of the oscillation correspondingly decreases ( $P \downarrow$ ). At the same time, the instantaneous phase angle decreases ( $\Delta\theta < 0$ ), corresponding to the decreased frequency of the oscillation ( $F \downarrow$ ).

Fig. 6 shows the joint amplitude-frequency modulation effect with phase index  $\phi$  increasing from 0 to 200ms. The frequency decreases and shows a clear periodicity (Fig. 6b), and the power shows a sinusoidal-like shape with the increase of the phase index  $\phi$  (Fig. 6c). The phase portrait with phase index  $\phi = 10, 45, 80, 115, 150$ , and 185 ms is illustrated in Fig. 6a. It is found that the increase of the trajectory radius ( $\Delta r > 0$ ) leads to the increase of power ( $P \uparrow$ ), and the increase of the instantaneous phase angle ( $\Delta\theta > 0$ ) corresponds to the increase of oscillation frequency ( $F \uparrow$ ).

#### 4.3. Modulation result with different parameters

Considering the background noise in the EEG signal, the noise-driven fixed-point attractor model is used to explore the influence of different parameter settings on alpha modulation results. These parameters are stimulation intensity, bandwidth and center frequency in the bandpass filter, and accuracy of phase estimation.

##### 4.3.1. Stimulation intensity

Fig. 7a shows how the modulation depth varies with stimulation intensity. The black line indicates the alpha amplitude without external stimulus, and the blue shade indicates the amplitude modulation range of the simulated alpha rhythm. The modulation depth increases with the stimulation intensity. More specifically, with the increase of stimulation intensity, the maximum amplitude of the modulated rhythm increases (upper bound of blue shadow). The minimum amplitude of the modulated rhythm (lower bound of blue shadow) first declines to reach the bottom at a stimulation intensity of 1000, and then rises with the stimulation intensity. With stimulation intensity greater than 3000, the suppression effect at certain phases in the PLVF no longer occurs. This result implies that, with the increase of stimulation intensity, the amplitude of alpha rhythm is more difficult to suppress. The frequency modulation effect shows that, with the increase of stimulation intensity, the peak frequency (bottom) is clearer and more focused, but the frequency modulation range remains unchanged (about 8–12 Hz).

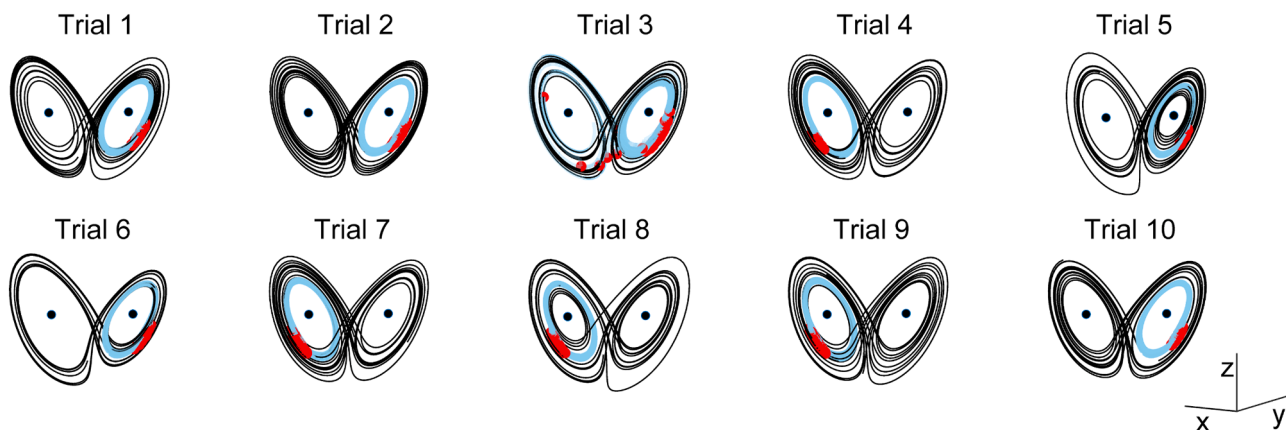


**Fig. 4.** The modulation results of different initial values with  $\phi = 70$ . The modulation curve converges to the left-wing, or the right-wing, which depends on the initial value.

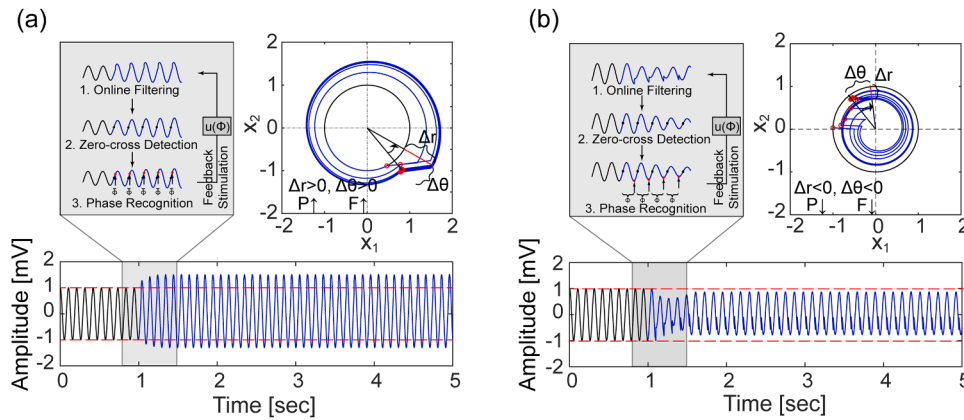


**Fig. 5.** Simulation results of PLVF system with external stimuli at phase index (time lag)  $\phi = 10$  ms (a) and at phase index (time lag)  $\phi = 80$  ms (b). Upper left in both (a) and (b): schema of output signal modulation. Black dots indicate the positive zero-crossing points. Red dots indicate the actual stimulation points. Upper right in both (a) and (b): modulation effect of the system in the phase space. Red dots indicate stimulation points. Angles of black arrows indicate angle changes of the system. Lower in both (a) and (b): output signals (simulated EEG signals). (For interpretation of the references to colour in this figure, the reader is referred to the web version of this article.)

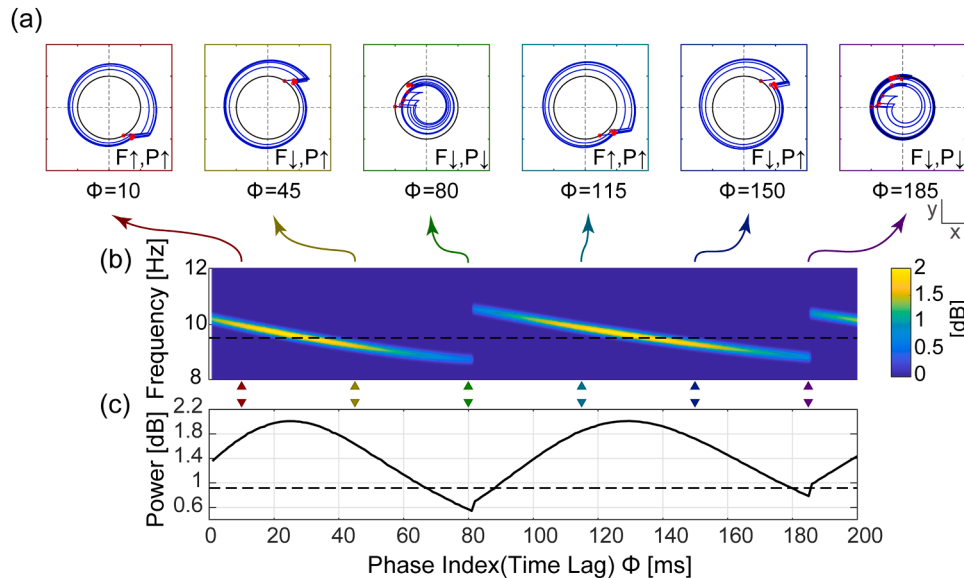


**Fig. 6.** Simulation results of the PLVF system with external stimuli as phase index (time lag)  $\phi$  increases from 0 to 200 ms. (a) Modulation effect of the system in the phase space, with phase index  $\phi$  of 10 ms, 45 ms, 80 ms, 115 ms, 150 ms, and 185 ms, respectively (left to right); (b) Power spectra of the system modulated by external stimuli delivered at different phases of  $\phi$ ; (c) Power modulation function against phase index  $\phi$ . Black-dashed lines indicate the frequency (b) or the power (c) without external stimuli.

#### 4.3.2. Bandwidth of bandpass filter

Fig. 7b shows the frequency modulation range with the change of filter bandwidth. The blue shade indicates the frequency modulation range of the simulated alpha rhythm, and the blue line indicates its peak frequency. Simulation results show that the frequency modulation range narrows as the filter bandwidth decreases. The frequency modulation results (bottom) with filter bandwidths of 6–16 Hz and 10–12 Hz are similar.

#### 4.3.3. Center frequency of bandpass filter

Fig. 7c shows the frequency modulation range with the change of center frequency of the bandpass filter. The frequency modulation range increases with the center frequency. The frequency modulation results (bottom) with filter bandwidths of 7–9 Hz and 11–13 Hz are similar.

#### 4.3.4. Accuracy of phase estimation

Fig. 7d shows that the modulation result varies with the phase estimation error index. Added random noise is increased with the increase of the phase index to control the phase estimation error. The red line indicates the curve of exponential fitting, which is fitted by the amplitude of alpha rhythm (black line) or the attenuation coefficient (black points). The absolute value of the attenuation coefficient increases with the phase estimation error index, which means the error of modulation increases with the phase estimation error index. The peak frequency gradually becomes ambiguous with the increase of the phase estimation

error index (from 0 to 0.5 at the bottom) and phase index (0–300 ms).

## 5. Discussion and conclusion

In this work, we investigated the dynamic mechanism of alpha rhythm via the simulation of the proposed PLVF protocol by Huang et al. (2019). All these investigations are conducive to our deeper understanding of the dynamic structure and modulation mechanism of alpha dynamics modulation in PLVF, which can have practical significance for the modulation of alpha oscillation and further be used for potentially be used cognitive enhancement and mental diseases treatment. In the following, we discuss the three questions raised in the section of introduction and provide our answers based on the results presented in this study.

### 5.1. What kind of alpha dynamic model exhibits a modulation phenomenon of PLVF?

In the proposing of PLVF, Huang et al. assumed the alpha oscillation as a simple pendulum (Huang et al., 2019). However, a simple pendulum is not a stable attractor, the joint amplitude-frequency modulation result was also not as expected. In this work, we firstly investigate what kind of alpha dynamic model would exhibit a similar modulation result. This work does not aim to seek a precise model in the simulation of alpha oscillation but to qualitatively explain what dynamic structure can

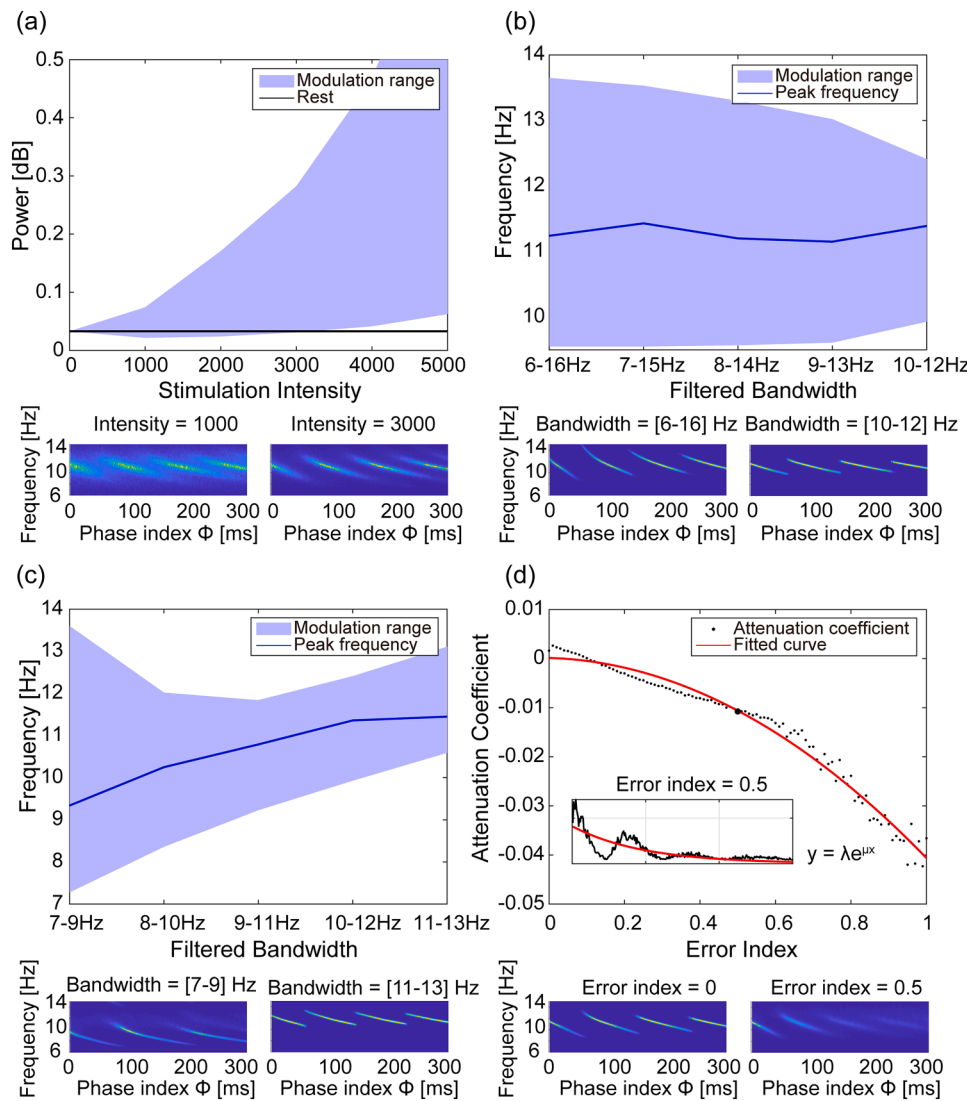


**Fig. 7.** Modulation results are affected by different factors: (a) stimulation intensity, (b) bandwidth of the bandpass filter, (c) center frequency of the bandpass filter, and (d) accuracy of phase estimation. (a) Upper: the result of modulation depth with the increase of stimulation intensity; Lower: frequency modulation results against phase index  $\phi$  with a stimulation intensity of 1000 or 3000. (b) Upper: the result of frequency modulation with the decrease of bandwidth of the bandpass filter (center frequency fixed at 11 Hz); Lower: frequency modulation result against phase index  $\phi$  with filter bandwidth of 6–16 Hz or 10–12 Hz. (c) Upper: the result of frequency modulation with the change of center frequency of the bandpass filter (bandwidth fixed at 2 Hz); Lower: frequency modulation result against phase index  $\phi$  with filter bandwidth of 7–9 Hz or 11–13 Hz. (d) Upper: attenuation index of amplitude modulation with the increase of error of phase estimation; Lower: frequency modulation result against phase index  $\phi$  with error index of 0 or 1.

produce such a modulation result by PLVF. Compare with the existing model, the actual alpha rhythm would be much more complex. The emphasis of mathematical modeling is not to consider all the details of the model but to abstract the core factors for the complex brain activity. Considering the large intra- and inter-subject variability, we did not make a precise estimation for the internal parameters in the model, but used the simplest models for all the three kinds of attractors to explore what kind of dynamic model exhibits a modulation phenomenon of PLVF?

Hence, the commonly used neural mass model and three well-studied attractors, including fixed-point attractor, limit-cycle attractor, and Lorenz strange attractor, were applied to simulate alpha oscillations and phase-locked feedback stimulation for alpha rhythm modulation. The simulation results show that the fixed-point attractor and the limit-cycle attractor are more consistent with the characteristics of real-world alpha dynamics. Both models have good global consistency, in that all points at different phases with the same radius have similar dynamic characteristics. They converge to a fixed point or a perfect circle by rotating at a fixed angular velocity. With the increase of the phase index  $\phi$ , the peak frequency of alpha rhythm decreases and has clear periodicity, and the power shows a sinusoidal-like shape. On the contrary, the strong nonlinearity in the neural mass model and Lorenz attractor would destroy this global consistency, which makes the amplitude and frequency responses of the PLVF simulation different from the real EEG

result.

## 5.2. What is the dynamic mechanism of PLVF for alpha modulation?

Based on the simple pendulum assumption, Huang et al. (2019) proposed the closed-loop PLVF method for the modulation of alpha oscillation. Entrained by the exogenous stimulus, a joint amplitude-frequency modulation was observed from the endogenous alpha oscillations. The amplitude modulation is consistent with the expectation of the model assumption, while the peak frequency modulation does not meet the expectation. Considering the real alpha dynamic is still somewhat a black box for researchers, the experiment result on the real EEG modulation may not promote the understanding of the dynamic mechanism of PLVF-based alpha modulation. Instead, a numerical simulation based on existing experimental results can help us further understand the dynamic mechanism for alpha modulation. Based on the simulation of the limit cycle model, we find that external stimulation at a specific phase can cause the stimulated EEG signal to stabilize on a new trajectory, which leads to the modulation of amplitude. More specifically, the change of the trajectory radius  $\Delta r$  modulated by external stimulation causes the modulation of alpha amplitude. With a constant angular velocity in the PLVF system, the change of instantaneous phase angle  $\Delta\theta$ , which is stimulated by external stimulation, gives rise to the change of peak frequency. As a result, the simultaneous

modulation of trajectory radius and instantaneous phase angle leads to the joint amplitude-frequency modulation of the alpha rhythm.

### 5.3. Which factors affect the modulation effects in PLVF?

The influences of stimulation intensity, bandwidth, and center frequency of the bandpass filter, and accuracy of phase estimation on the modulation result are investigated. The modulation effect of the simulated alpha rhythm is affected by the stimulus intensity and the filter bandwidth. More precisely, the modulation effect on alpha amplitude is mainly affected by stimulus intensity, while the modulation effect on peak frequency is mainly influenced by filter bandwidth. It is worth noting that the suppression effect of the amplitude would disappear when the stimulus intensity is increased to a certain extent. The phenomenon can be explained by the limit-cycle attractor. When the change of trajectory radius  $\Delta r$  caused by external stimuli is greater than the radius of the initial trajectory, external stimuli only causes a promoting effect on the amplitude of the alpha rhythm (in Fig. 7a, the promoting effect is indicated by the blue shade above the black line, and the suppression effect is indicated by the blue shade below the black line). In addition, the accuracy of phase estimation directly affects that of the modulation result, which means the accuracy of phase estimation is fundamental to EEG modulation.

In conclusion, the results of this study provide us with greater insights into alpha rhythm modulation. By comparing four types of dynamic models in the simulation of PLVF modulation, we find that the dynamic evolution of alpha rhythm may follow a simpler dynamic structure (a fixed-point attractor or a limit-cycle attractor with globally consistent dynamic characteristics). In contrast to the highly complex functions of the brain, this result indicates that the dynamic structure of alpha rhythm may be much simpler than our expected, which even simpler than the greatly simplified lumped neural mass model. Further simulation results also explain the dynamic mechanism of PLVF for amplitude and frequency modulation of alpha rhythm and how did the parameters in the model simulation influence the modulation result. All these investigations are not only helpful for the in-depth understanding of alpha oscillation and the dynamic mechanism of PLVF modulation, but also provide theoretical guidance for the development of a precise, effective, and controllable neuromodulation technology. More specifically, the result of this study suggests that to achieve the goal of increasing or decreasing alpha rhythm, different modulation strategies should be designed. Increasing the alpha amplitude can be simply achieved by increasing the stimulation intensity in PLVF modulation, while the suppression of the alpha amplitude is more difficult, which depends on the phase of stimulation at certain intervals of the stimulation intensity.

For future work, it should be noticed that the investigation of the EEG dynamics is limited on the alpha oscillation. Currently, the modulation with PLVF methods has only been verified on the alpha band oscillation by the visual stimulus on the occipital area. Several meaningful topics need to be explored.

- Other sensory stimuli.** Based on the evidence for steady-state visual/ somatosensory/ auditory evoked potential (SSVEP/ SSSEP/ SSAEP), the visual, vibrotactile and auditory stimulus would have the largest response from their corresponding primary sensory cortex, at the frequency band around 10 Hz, 20 Hz, and 40 Hz correspondingly (Northoff et al., 2010). Whether PLVF modulation would be extended to the other band, other brain areas by other types of stimulus, and how about the neural dynamic for the modulation would be interesting to explore.

- Other stimulation techniques.** PLVF modulates the brain rhythm along the sensory pathway. Unlike the other noninvasive brain stimulation technique, like TMS, TDCS, and TACS, PLVF could not effectively work on any target brain area. But artifact-free is the most significant characteristic for PLVF modulation. Based on this, closed-

looped modulation is easy to develop by decoding the brain signal in real-time. The large artifact in TMS, TDCS, and TACS, by contrast, would make the closed-looped modulation difficult or indirectly (Noury and Siegel, 2017; Noury et al., 2016), which is considered as one of the main reasons for inter-subject variability (Frohlich and Townsend, 2021).

- Other brain rhythms.** The current work focuses on the alpha rhythm modulation with eyes open. In 2020, Philipp et al. (Philipp, 2018) reported a consistent result in the modulation of alpha rhythm with eyes closed, which demonstrates effective of the PLVF method on close eye alpha rhythm modulation. Whether the result of alpha dynamic analysis still works on other sub-bands, especially the gamma band, still needs to be verified. Gamma rhythm may have very different functions and dynamics from alpha rhythm (Herrmann and Demiralp, 2005; Le Van Quyen and Bragin, 2007). The cross-frequency coupling between gamma and theta oscillation might play a functional role in inter-cortical communication computation, and learning (Canolty and Knight, 2010; Jensen and Colgin, 2007). Recent studies show the links between gamma and cognitive functions, such as emotion (Aydin et al., 2016; Aydin, 2020), working memory (Howard et al., 2003). However, the low amplitude and high oscillation of the gamma rhythm make it difficult to be modulated by phase-locked feedback stimulus.
- Other brain functions.** The proposed PLVF could modulate the alpha oscillation on the primary sensory cortex with eyes open. How to further modulate the cognitive related brain rhythm and further affect users' cognition and behavior need to be further explored, which should be rigorously examined by well-designed experiments, large-scale validation, randomized trials, and longitudinal study, and be compared with other types of mainstream and advanced brain stimulation techniques.

### Acknowledgments

This work was supported by the Science, Technology, and Innovation Commission of Shenzhen Municipality Technology Fund (No. JCYJ20190808173819182, JCYJ20170818093322718), the Shenzhen Science and Technology Program (No. JSGG20210713091811038), and the National Natural Science Foundation of China (No. 81871443). None of the authors has potential conflicts of interest to be disclosed.

### Declaration of Interest Statement

None.

### References

- Aydin, S., 2020. Deep learning classification of neuro-emotional phase domain complexity levels induced by affective video film clips. *IEEE J. Biomed. Health Inform.* 24, 1695–1702.
- Aydin, S., Demirtas, S., Ates, K., Tunga, M.A., 2016. Emotion recognition with eigen features of frequency band activities embedded in induced brain oscillations mediated by affective pictures. *Int. J. Neural Syst.* 26, 1650013.
- Beliaeva, V., Savvateev, I., Zerbi, V., Polania, R., 2021. Toward integrative approaches to study the causal role of neural oscillations via transcranial electrical stimulation. *Nat. Commun.* 12, 2243.
- Bollimunta, A., Mo, J., Schroeder, C.E., Ding, M., 2011. Neuronal mechanisms and attentional modulation of corticothalamic alpha oscillations. *J. Neurosci.* 31, 4935–4943.
- Brandt, M.E., 1997. Visual and auditory evoked phase resetting of the alpha EEG. *Int. J. Psychophysiol.* 26, 285–298.
- Butnik, S.M., 2005. Neurofeedback in adolescents and adults with attention deficit hyperactivity disorder. *J. Clin. Psychol.* 61, 621–625.
- Canolty, R.T., Knight, R.T., 2010. The functional role of cross-frequency coupling. *Trends Cogn. Sci.* 14, 506–515.
- Choi, S.W., Chi, S.E., Chung, S.Y., Kim, J.W., Ahn, C.Y., Kim, H.T., 2011. Is alpha wave neurofeedback effective with randomized clinical trials in depression? a pilot study. *Neuropsychobiology* 63, 43–51.
- Cohen, M.X., 2017. Where does EEG come from and what does it mean? *Trends Neurosci.* 40, 208–218.
- Debener, S., Ullsperger, M., Siegel, M., Engel, A.K., 2006. Single-trial EEG-fMRI reveals the dynamics of cognitive function. *Trends Cogn. Sci.* 10, 558–563.

- Fox, D.J., Tharp, D.F., Fox, L.C., 2005. Neurofeedback: an alternative and efficacious treatment for attention deficit hyperactivity disorder. *Appl. Psychophysiol. Biofeedback* 30, 365–373.
- Frohlich, F., Townsend, L., 2021. Closed-loop transcranial alternating current stimulation: towards personalized non-invasive brain stimulation for the treatment of psychiatric illnesses. *Curr. Behav. Neurosci. Rep.* 8, 51–57.
- Glass, L., Kaplan, D.T., Lewis, J.E., 1993. Tests for deterministic dynamics in real and model neural networks. In: Proceedings of the 2nd Annual Conference on Nonlinear Dynamics Analysis of the EEG, World Scientific, Singapore. pp. 223–249.
- Grandy, T.H., Werkle-Bergner, M., Chicherio, C., Schmiedek, F., Loevden, M., Lindenberger, U., 2013. Peak individual alpha frequency qualifies as a stable neurophysiological trait marker in healthy younger and older adults. *Psychophysiology* 50, 570–582.
- Grimbert, F., Faugeras, O., 2006. Bifurcation analysis of Jansen's neural mass model. *Neural Comput.* 18, 3052–3068.
- Halgren, M., Ulbert, I., Bastuji, H., Fabó, D., Eröss, L., Rey, M., Devinsky, O., Doyle, W.K., Mak-McCully, R., Halgren, E., Wittner, L., Chauvel, P., Heit, G., Eskandar, E., Mandell, A., Cash, S.S., 2019. The generation and propagation of the human alpha rhythm. *Proc. Natl. Acad. Sci.* 116, 23772–23782.
- Hammond, D.C., 2005. Neurofeedback treatment of depression and anxiety. *J. Adult Dev.* 12, 131–137.
- Hanslmayr, S., Sauseng, P., Doppelmayr, M., Schabus, M., Klimesch, W., 2005. Increasing individual upper alpha power by neurofeedback improves cognitive performance in human subjects. *Appl. Psychophysiol. Biofeedback* 30, 1–10.
- Hanslmayr, S., Gross, J., Klimesch, W., Shapiro, K.L., 2011. The role of alpha oscillations in temporal attention. *Brain Res. Rev.* 67, 331–343.
- Herrmann, C.S., Demiralp, T., 2005. Human EEG gamma oscillations in neuropsychiatric disorders. *Clin. Neurophysiol.* 116, 2719–2733.
- Howard, M.W., Rizzuto, D.S., Caplan, J.B., Madsen, J.R., Lisman, J., Aschenbrenner-Scheibe, R., Schulze-Bonhage, A., Kahana, M.J., 2003. Gamma oscillations correlate with working memory load in humans. *Cereb. Cortex* 13, 1369–1374.
- Hsueh, J.J., 2017. Neurofeedback training of EEG alpha rhythm enhances episodic and working memory (vol 37, pg 2662, 2016). *Hum. Brain Mapp.* 38, 3315.
- Huang, G., Zhang, D., Meng, J., Zhu, X., 2011. Interactions between two neural populations: a mechanism of chaos and oscillation in neural mass model. *Neurocomputing* 74, 1026–1034.
- Huang, G., Liu, J., Li, L., Zhang, L., Zeng, Y., Ren, L., Ye, S., Zhang, Z., 2019. A novel training-free externally-regulated neurofeedback (ER-NF) system using phase-guided visual stimulation for alpha modulation. *Neuroimage* 189, 688–699.
- Ince, R., Adanir, S.S., Sevmez, F., 2020. The inventor of electroencephalography (EEG). *Childs Nervous System*. Hans Berger, pp. 1873–1941.
- Jansen, B.H., Rit, V.G., 1995. Electroencephalogram and visual evoked potential generation in a mathematical model of coupled cortical columns. *Biol. Cybern.* 73, 357–366.
- Jansen, B.H., Zouridakis, G., Brandt, M.E., 1993. A neurophysiologically-based mathematical model of flash visual evoked potentials. *Biol. Cybern.* 68, 275–283.
- Jensen, O., Colgin, L.L., 2007. Cross-frequency coupling between neuronal oscillations. *Trends Cogn. Sci.* 11, 267–269.
- Kasten, F.H., Herrmann, C.S., 2019. Recovering brain dynamics during concurrent tACS-M/EEG: an overview of analysis approaches and their methodological and interpretational pitfalls. *Brain Topogr.* 32, 1013–1019.
- Kirschfeld, K., 2005. The physical basis of alpha waves in the electroencephalogram and the origin of the “Berger effect”. *Biol. Cybern.* 92, 177–185.
- Le Van Quyen, M., Bragin, A., 2007. Analysis of dynamic brain oscillations: methodological advances. *Trends Neurosci.* 30, 365–373.
- Lopes da Silva, F.H., Vos, J.E., Mooibroek, J., Vanrotterdam, A., 1980. Relative contributions of intracortical and thalamo-cortical processes in the generation of alpha rhythms, revealed by partial coherence analysis. *Electroencephalogr. Clin. Neurophysiol.* 50, 449–456.
- Lopes da Silva, F.H., Pijn, J.P., Velis, D., Nijssen, P.C.G., 1997. Alpha rhythms: noise, dynamics and models. *Int. J. Psychophysiol.* 26, 237–249.
- Maltseva, I.V., Masllobœuf, Y.P., 1997. Alpha rhythm parameters and short-term memory span. *Int. J. Psychophysiol.* 27, 169–180.
- Mansouri, F., Fettes, P., Schulze, L., Giacobbe, P., Zariffa, J., Downar, J., 2018. A real-time phase-locking system for non-invasive brain stimulation. *Front. Neurosci.* 12, 877.
- Northoff, G., Qin, P.M., Nakao, T., 2010. Rest-stimulus interaction in the brain: a review. *Trends Neurosci.* 33, 277–284.
- Noury, N., Siegel, M., 2017. Phase properties of transcranial electrical stimulation artifacts in electrophysiological recordings. *Neuroimage* 158, 406–416.
- Noury, N., Hipp, J.F., Siegel, M., 2016. Physiological processes non-linearly affect electrophysiological recordings during transcranial electric stimulation. *Neuroimage* 140, 99–109.
- Palus, M., 1993. Testing for nonlinearity in the EEG. In: Proceedings of the 2nd Annual Conference on Nonlinear Dynamical Analysis of the EEG, World Scientific, Singapore. pp. 100–14.
- Pereda, E., Quiroga, R.Q., Bhattacharya, J., 2005. Nonlinear multivariate analysis of neurophysiological signals. *Prog. Neurobiol.* 77, 1–37.
- Philipp, S., 2018. Closed-loop photic stimulation using EEG. *Neuropsychobiology* 77, 155.
- Schreckenberger, M., Lange-Asschenfeldt, C., Lochmann, M., Mann, K., Siessmeier, T., Buchholz, H.G., Bartenstein, P., Gründer, G., 2006. The thalamus as the generator and modulator of EEG alpha rhythm: a combined PET/EEG study with lorazepam challenge in humans. *Neuroimage* 32, 485.
- Schwab, K., Ligges, C., Jungmann, T., Hilgenfeld, B., Haueisen, J., Witte, H., 2006. Alpha entrainment in human electroencephalogram and magnetoencephalogram recordings. *Neuroreport* 17, 1829–1833.
- Stam, C.J., Pijn, J.P.M., Suffczynski, P., Lopes da Silva, F.H., 1999. Dynamics of the human alpha rhythm: evidence for non-linearity? *Clin. Neurophysiol.* 110, 1801–1813.
- Vijayan, S., Kopell, N.J., 2012. Thalamic model of awake alpha oscillations and implications for stimulus processing. *Proc. Natl. Acad. Sci.* 109, 18553–18558.
- Zarubin, G., Gundlach, C., Nikulin, V., Villringer, A., Bogdan, M., 2020. Transient amplitude modulation of alpha-band oscillations by short-time intermittent closed-loop tACS. *Front. Hum. Neurosci.* 14, 366.
- Zhang, L., 2017. Artificial neural networks model design of Lorenz chaotic system for EEG pattern recognition and prediction. In: Proceeding of IEEE Life Science Conference. pp. 39–42.